

Measuring the distance-redshift relation with the cross-correlation of gravitational wave standard sirens and galaxies

Masamune Oguri^{1,2,3}¹*Research Center for the Early Universe, University of Tokyo, Tokyo 113-0033, Japan*²*Department of Physics, University of Tokyo, Tokyo 113-0033, Japan*³*Kavli Institute for the Physics and Mathematics of the Universe (Kavli IPMU, WPI),**University of Tokyo, Chiba 277-8582, Japan*

(Received 10 March 2016; published 13 April 2016)

Gravitational waves from inspiraling compact binaries are known to be an excellent absolute distance indicator, yet it is unclear whether electromagnetic counterparts of these events are securely identified for measuring their redshifts, especially in the case of black hole–black hole mergers such as the one recently observed with the Advanced LIGO. We propose to use the cross-correlation between spatial distributions of gravitational wave sources and galaxies with known redshifts as an alternative means of constraining the distance-redshift relation from gravitational waves. In our analysis, we explicitly include the modulation of the distribution of gravitational wave sources due to weak gravitational lensing. We show that the cross-correlation analysis in next-generation observations will be able to tightly constrain the relation between the absolute distance and the redshift and therefore constrain the Hubble constant as well as dark energy parameters.

DOI: [10.1103/PhysRevD.93.083511](https://doi.org/10.1103/PhysRevD.93.083511)

I. INTRODUCTION

The observation of the gravitational wave (GW) signal GW150914 by the Advanced Laser Interferometer Gravitational Wave Observatory (LIGO) opened up the possibility of using GWs as cosmological and astrophysical probes [1–3]. GW150914 is a GW signal from a pair of merging black holes (BHs) at $z \sim 0.1$, with a mass of each BH of $M \sim 30M_{\odot}$, which were inferred by fitting the observed waveform with numerical relativity waveforms. The discovery of such a BH–BH merger event implies that BH–BH mergers may be much more ubiquitous than previously thought.

GWs from inspiraling compact binaries, which are sometimes referred to as standard sirens, are potentially a very powerful cosmological probe, because they can determine the absolute distances to the GW sources [4]. Assuming general relativity, one can obtain information on masses of inspiraling and merging objects from the shape of the waveform, which then determines the absolute strain amplitude of GWs emitted from these objects. Thus, the comparison of the observed strain amplitude enables a direct measurement of the luminosity distance to the GW source. Indeed, the luminosity distance to GW150914 was estimated to be 410_{-180}^{+160} Mpc using this technique [1]. With the redshift information from independent observations of an electromagnetic (EM) counterpart, one can directly constrain the absolute distance-redshift relation and hence obtain constraints on cosmological parameters including the Hubble constant and dark energy parameters [5–16].

However, it is unclear whether EM counterparts can really be observed. In the case of GW150914, while a hard

x-ray emission that might possibly be associated with GW150914 was detected with the Fermi Gamma-ray Burst Monitor [17], no confirmed EM counterpart is reported. Since mergers of BHs are not expected to have EM counterparts, this association of the hard x-ray emission, if real, requires special explanations such as a BH–BH merger in a dense environment (e.g., [18]). If a bulk of BH–BH mergers do not have EM counterparts, their use as a cosmological probe will be limited.

It has been argued that GWs from compact binary mergers would be useful even if EM counterparts are not identified. Nishizawa *et al.* [19] discussed the possibility of exploiting the phase shift [20] of binary sources to constrain cosmological parameters without EM counterparts. Messenger and Read [21] proposed to use tidal effects on merging neutron stars to break the degeneracy to obtain information on the redshift of the system. Another approach is to take advantage of the clustering property of GW sources. Recently, Namikawa *et al.* [22] showed that the large-angle autocorrelation of GW sources can provide tight constraints on primordial non-Gaussianity.

In this paper, we propose the cross-correlation between spatial distributions of compact binary GW sources without redshift information and a galaxy sample with known redshifts as a new method to extract cosmological information from GWs. We show that this cross-correlation extracts information on the distance-redshift relation and hence constrains cosmological parameters including the Hubble constant that determines the absolute distance scale. This is made possible because the cross-correlation signal is maximized when luminosity distances of GW sources and redshifts of the galaxy sample matches.

The idea is similar to the cross-correlation of photometric and spectroscopic galaxies to calibrate photometric redshifts of galaxies [23]. A complication is that luminosity distances estimated from GWs are affected by weak gravitational lensing, which induces additional spatial correlations on the sky (e.g., [15,22]). In this paper, we explicitly include this effect in our formulation.

This paper is organized as follows. In Sec. II, we give our formulation. We present our result including the Fisher matrix analysis in Sec. III. Finally we give our conclusion in Sec. IV. Our fiducial cosmological model is based on the latest Planck result [24] and has matter density $\Omega_m = 0.308$, dark energy density $\Omega_{de} = 0.692$, baryon density $\Omega_b = 0.04867$, the dimensionless Hubble constant $h = 0.6763$, the spectral index 0.9677, the normalization of matter fluctuations $\sigma_8 = 0.815$, and dark energy equation of state $w_{de} = -1$. Throughout the paper, we assume a flat universe.

II. AUTO- AND CROSS-CORRELATIONS OF GRAVITATIONAL WAVE SOURCES

A. Distance to gravitational wave sources

Observations of GWs from mergers of compact binaries provide information on luminosity distances D to the GW sources. On the other hand, their redshifts are not a direct observable. In this paper, for simplicity, we assume that the observed luminosity distance D_{obs} from the analysis of the waveform is related to the true distance D via the log-normal distribution

$$p(D_{\text{obs}}|D) = \frac{1}{\sqrt{2\pi}\sigma_{\ln D}} \exp[-x^2(D_{\text{obs}})] \frac{1}{D_{\text{obs}}}, \quad (1)$$

where

$$x(D_{\text{obs}}) \equiv \frac{\ln D_{\text{obs}} - \ln D}{\sqrt{2}\sigma_{\ln D}}. \quad (2)$$

The dispersion on D_{obs} is caused by various effects, including the statistical error of GW observations and the degeneracy of the luminosity distance with other parameters such as masses of compact objects and the inclination of the system. The parameter $\sigma_{\ln D}$ quantifies the dispersion. Considering Einstein Telescope [25] like GW observations, in this paper we assume the dispersion of the distance estimate of $\sigma_{\ln D} = 0.05$ (e.g., [15]). In addition, weak gravitational lensing also affects cosmological distances. We include the effect of weak gravitational lensing explicitly by relating the distance D to the average distance \bar{D} , which represents the standard luminosity distance computed from the homogeneous and isotropic Friedmann-Robertson-Walker universe, as

$$D = \bar{D}\mu^{-1/2} \approx \bar{D}[1 - \kappa(\boldsymbol{\theta}, z)], \quad (3)$$

where $\kappa(\boldsymbol{\theta}, z)$ is the lensing convergence, which is a function of the sky position $\boldsymbol{\theta}$ and redshift z . The lensing convergence is essentially a projected matter density field, and is given by

$$\begin{aligned} \kappa(\boldsymbol{\theta}, z) &= \int_0^z dz' \frac{\bar{\rho}_m(z')}{H(z')(1+z')\Sigma_{\text{crit}}(z'; z)} \delta_m(\boldsymbol{\theta}, z) \\ &\equiv \int_0^z dz' W^\kappa(z'; z) \delta_m(\boldsymbol{\theta}, z'), \end{aligned} \quad (4)$$

where $\delta_m(\boldsymbol{\theta}, z)$ is the matter density field, $H(z)$ is the Hubble parameter, $\Sigma_{\text{crit}}(z; z_s)$ is the (physical) critical surface density at redshift z' for the source redshift z , and $\bar{\rho}_m(z) = \Omega_m \rho_{\text{cr},0} (1+z)^3$ is a mean physical density of the Universe at redshift z .

B. Projected density field of gravitational wave sources

We construct the i th angular density field of GW sources by projecting them in the luminosity distance range $D_{\text{min},i} < D_{\text{obs}} < D_{\text{max},i}$. Given the log-normal relation between the observed and true distances, the angular number density is computed from the three-dimensional number density field of GW sources $n_{\text{GW}}(\boldsymbol{\theta}, z)$ as

$$n_i^{\text{w}}(\boldsymbol{\theta}) = \int_0^\infty dz \frac{\chi^2}{H(z)} S_i(z) n_{\text{GW}}(\boldsymbol{\theta}, z), \quad (5)$$

where the comoving angular diameter distance is $\chi = \int_0^z dz' [1/H(z')]$ and $S_i(z)$ describes the selection function along the line-of-sight

$$S_i(z) \equiv \frac{1}{2} [\text{erfc}\{x(D_{i,\text{min}})\} - \text{erfc}\{x(D_{i,\text{max}})\}]. \quad (6)$$

The average projected number density of GW sources in the i th bin is

$$\begin{aligned} \bar{n}_i^{\text{w}} &= \int_0^\infty dz \frac{\chi^2}{H(z)} S_i(z) \bar{n}_{\text{GW}}(z) \\ &= \int_0^\infty dz \frac{\chi^2}{H(z)} S_i(z) T_{\text{obs}} \frac{\dot{n}_{\text{GW}}(z)}{1+z}. \end{aligned} \quad (7)$$

Here T_{obs} is the duration of the observation and $\dot{n}_{\text{GW}}(z)$ is the rate of merger events that can be observed with GW detectors of interest. The factor $1+z$ in the denominator accounts for the cosmological time dilation effect.

The merger rate $\dot{n}_{\text{GW}}(z)$ has not yet been constrained very well. The observation of GW150914 implies the BH-BH merger rate of $\dot{n}_{\text{GW}} \sim 10^{-6} - 10^{-8} h^3 \text{ Mpc}^{-3} \text{ yr}^{-1}$ at the local Universe [2]. Several models predict that the BH-BH merger rate increases toward higher redshifts (e.g., [26–28]). We can also use GWs from neutron star mergers for our cross-correlation study, and their rate is estimated

to be of similar order. Thus in this paper we assume $T_{\text{obs}}\dot{n}_{\text{GW}} = 3 \times 10^{-6} h^3 \text{ Mpc}^{-3}$ over all the redshift range of our interest.

The expression of the projected number density $n_i^w(\boldsymbol{\theta})$ allows us to define the projected density field $\delta_i^{2\text{D},w}(\boldsymbol{\theta})$, which plays a central role in our cross-correlation analysis. While the main fluctuation comes from the three-dimensional distribution of GW sources, $n_{\text{GW}}(\boldsymbol{\theta}, z) = \bar{n}_{\text{GW}}(z)[1 + \delta_{\text{GW}}(\boldsymbol{\theta}, z)]$, the convergence in Eq. (3) induces additional spatial fluctuations. Assuming that $\kappa(\boldsymbol{\theta}, z)$ is sufficiently small, we obtain

$$\begin{aligned} \delta_i^{2\text{D},w}(\boldsymbol{\theta}) &\equiv \frac{n_i^w(\boldsymbol{\theta}) - \bar{n}_i^w}{\bar{n}_i^w} \\ &\approx \frac{1}{\bar{n}_i^w} \int_0^\infty dz \frac{\chi^2}{H(z)} \bar{n}_{\text{GW}}(z) S_i(z) \delta_{\text{GW}}(\boldsymbol{\theta}, z) \\ &\quad + \frac{1}{\bar{n}_i^w} \int_0^\infty dz \frac{\chi^2}{H(z)} \bar{n}_{\text{GW}}(z) T_i(z) \kappa(\boldsymbol{\theta}, z), \\ &\equiv \int_0^\infty dz [W_i^s(z) \delta_{\text{GW}}(\boldsymbol{\theta}, z) + W_i^t(z) \kappa(\boldsymbol{\theta}, z)], \end{aligned} \quad (8)$$

where

$$T_i(z) \equiv \frac{-\exp[-x^2(D_{i,\text{min}})] + \exp[-x^2(D_{i,\text{max}})]}{\sqrt{2\pi}\sigma_{\ln D}}. \quad (9)$$

The first term of Eq. (8) describes the intrinsic spatial inhomogeneity of GW sources, whereas the second term of Eq. (8) comes from the apparent modulation of the distribution of GW sources on the sky due to weak gravitational lensing which changes luminosity distances inferred from waveforms. Eq. (9) implies that the second term of Eq. (8) is smaller than the first term, but as we will show later, the second term can make dominate contributions to correlation signals, because the convergence contains accumulated information along the line-of-sight.

C. Angular correlation

For simplicity, we assume a linear bias $\delta_{\text{GW}} = b_{\text{GW}}\delta_m$ for GW sources. This assumption is reasonable in the sense that mergers of compact binary objects are expected to be associated with galaxies which are known to trace large-scale structure of the Universe. The angular power spectrum of the density field $\delta_i^{2\text{D},w}(\boldsymbol{\theta})$ in Eq. (8) between i th and j th bins is calculated using the Limber's approximation [29,30] as

$$C^{w_i w_j}(\ell) = C^{s_i s_j}(\ell) + C^{s_i t_j}(\ell) + C^{s_j t_i}(\ell) + C^{t_i t_j}(\ell), \quad (10)$$

$$C^{s_i s_j}(\ell) = \int_0^\infty dz W_i^s(z) W_j^s(z) \frac{H(z)}{\chi^2} b_{\text{GW}}^2 P_m\left(\frac{\ell + 1/2}{\chi}; z\right), \quad (11)$$

$$\begin{aligned} C^{s_i t_j}(\ell) &= \int_0^\infty dz W_j^t(z) \int_0^z dz' W_i^s(z') W^\kappa(z'; z) \\ &\quad \times \frac{H(z')}{\chi'^2} b_{\text{GW}} P_m\left(\frac{\ell + 1/2}{\chi'}; z'\right), \end{aligned} \quad (12)$$

$$\begin{aligned} C^{t_i t_j}(\ell) &= \int_0^\infty dz W_i^t(z) \int_0^\infty dz' W_j^t(z') \int_0^{\min(z, z')} dz'' \\ &\quad \times W^\kappa(z''; z) W^\kappa(z''; z') \frac{H(z'')}{\chi''^2} P_m\left(\frac{\ell + 1/2}{\chi''}; z''\right), \end{aligned} \quad (13)$$

where $P_m(k; z)$ is the matter power spectrum. Since we are interested in relatively large angular scales ($\ell \lesssim 300$), the cross spectrum is dominated by the so-called two-halo term (see, e.g., [31]), which suggests that we can use the linear matter power spectrum for $P_m(k; z)$ in $C^{s_i s_j}$ and $C^{s_i t_j}$. On the other hand, $C^{t_i t_j}$ is given by a projection of all matter fluctuations along the line-of-sight which mixes small and large scale fluctuations. Thus it may be more appropriate to use the nonlinear matter power spectrum for $P_m(k; z)$ in $C^{t_i t_j}$. In this paper, we compute the transfer function of the linear matter power spectrum using the result in [32], and the nonlinear matter power spectrum using the result in [33].

D. Cross-correlation with spectroscopic galaxies

Next we consider a spectroscopic galaxy sample in the i th bin defined by the redshift range $z_{\text{min},i} < z < z_{\text{max},i}$

$$\delta_i^{2\text{D},g}(\boldsymbol{\theta}) = \int_0^\infty dz W_i^g(z) \delta_g(\boldsymbol{\theta}, z), \quad (14)$$

where

$$W_i^g(z) \equiv \frac{1}{\bar{n}_i^g} \frac{\chi^2}{H(z)} \bar{n}_g(z) \Theta(z - z_{\text{min},i}) \Theta(z_{\text{max},i} - z). \quad (15)$$

Here the three-dimensional comoving number density of the spectroscopic galaxy sample is denoted by $\bar{n}_g(z)$, and the average projected number density in the i th bin is simply computed as

$$\bar{n}_i^g = \int_0^\infty dz W_i^g(z). \quad (16)$$

In this paper, we simply assume a constant number density of $\bar{n}_g = 10^{-3} h^3 \text{ Mpc}^{-3}$ which resembles, e.g., a spectroscopic galaxy sample obtained by Euclid [34]. Using the Limber's approximation, the angular power spectrum of spectroscopic galaxies between i th and j th bins is given by

$$C^{g_i g_j}(\ell) = \delta_{ij} \int_0^\infty dz [W_i^g(z)]^2 \frac{H(z)}{\chi^2} b_g^2 P_m\left(\frac{\ell + 1/2}{\chi}; z\right), \quad (17)$$

where we assumed that there is no overlap of redshift ranges between different redshift bins, and b_g is the bias parameter for the spectroscopic galaxies.

We now consider the cross-correlation between the GW sources and the spectroscopic galaxies. From Eq. (8), we can compute the cross-correlation power spectrum as

$$C^{w_i g_j}(\ell) = C^{s_i g_j}(\ell) + C^{l_i g_j}(\ell), \quad (18)$$

$$C^{s_i g_j}(\ell) = \int_0^\infty dz W_i^s(z) W_j^g(z) \frac{H(z)}{\chi^2} \times b_{\text{GW}} b_g P_m \left(\frac{\ell + 1/2}{\chi}; z \right), \quad (19)$$

$$C^{l_i g_j}(\ell) = \int_0^\infty dz W_i^l(z) \int_0^z dz' W_j^g(z') W^k(z'; z) \times \frac{H(z')}{\chi'^2} b_g P_m \left(\frac{\ell + 1/2}{\chi'}; z' \right). \quad (20)$$

We use the linear power spectrum for $P_m(k; z)$ in both $C^{s_i g_j}$ and $C^{l_i g_j}$. The power spectrum $C^{s_i g_j}$ comes from the first term of Eq. (8) and represents the physical correlation of spatial distributions. On the other hand, $C^{l_i g_j}$, which comes from the second term of Eq. (8), is the correlation of the weak lensing effect on luminosity distances of GW sources with spectroscopic galaxies. Since all matter fluctuations along the line-of-sight contributes to weak lensing, it induces non-negligible cross-correlations between luminosity and redshift bins which are well separated with each other.

III. RESULT

A. Cross-correlation signal

First it is useful to study the cross angular power spectrum $C^{w_i g_j}(\ell)$ which is defined in Eq. (18). We fix the luminosity distance bin of GW sources to that corresponds to $0.9 < z < 1.1$ in our fiducial cosmological model. On the other hand, we move the central redshift of the spectroscopic galaxy sample while fixing the bin width to $\Delta z = 0.1$ in order to see how the cross-correlation signal changes as a function of the redshift of the spectroscopic galaxy sample. For bias parameters, we assume a simple parametric form $b_{\text{GW}}(z) = b_{w1} + b_{w2}/D(z)$ and $b_g = b_{g1} + b_{g2}/D(z)$, where $D(z)$ is the linear growth rate, and choose fiducial parameter values as $b_{w1} = b_{w2} = 1$ and $b_{g1} = b_{g2} = 1$.

Fig. 1 shows the cross-correlation power spectrum at multiple $\ell = 100$ as a function of the central redshift of the spectroscopic galaxy sample z_g . When the redshift of the spectroscopic galaxy sample well overlaps with that of GW sources, the cross-correlation signal becomes large. In this case, the cross-correlation signal is dominated by the physical correlation of density fields of GW sources and

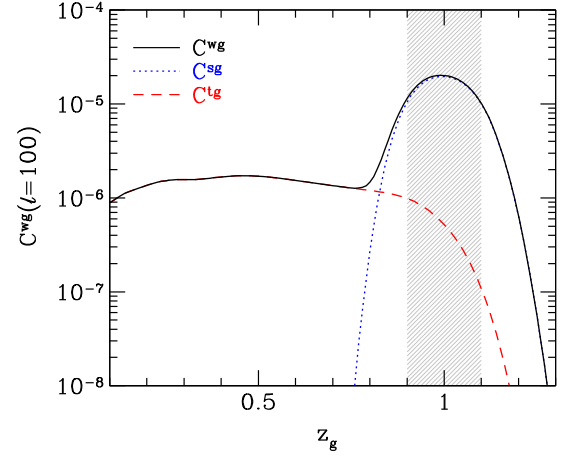


FIG. 1. The cross-correlation power spectrum C^{wg} between GW sources and galaxies [Eq. (18)]. The luminosity distance range of GW sources is fixed to that corresponds to $0.9 < z < 1.1$ (gray shaded region) in our fiducial cosmology. The spectroscopic galaxy sample has the redshift range $z_g - \Delta z/2 < z < z_g + \Delta z/2$ with $\Delta z = 0.1$. Solid line shows the cross-correlation power spectrum at multipole $\ell = 100$ as a function of the central redshift of the galaxy sample z_g . Dotted and dashed lines show contributions of C^{sg} [Eq. (19)] and C^{lg} [Eq. (20)] to C^{wg} , respectively.

spectroscopic galaxies, which corresponds to C^{sg} defined in Eq. (19). The cross-correlation signal is maximized when the luminosity distance bin best matches with the redshift bin, from which we can infer the relation between the luminosity distance and redshift. However, Fig. 1 indicates that the cross-correlation signal extend to much lower redshift of the spectroscopic galaxy sample. This extra correlation originates from C^{lg} defined in Eq. (20). As stated above, this term represents the correlation of galaxies and matter fluctuations along the line-of-sight that induces weak gravitational lensing effect on luminosity distances of GW sources. We include this large-distance cross-correlations in our Fisher matrix analysis below.

B. Fisher matrix analysis

Here we estimate how well we can constrain the distance-redshift relation and hence cosmological parameters from the cross-correlation analysis. For this purpose we need the covariance matrix of auto- and cross-correlation power spectra. Assuming Gaussian statistics, the covariance matrix is given by

$$\text{Cov}[C^{ij}(\ell), C^{mn}(\ell')] = \frac{4\pi}{\Omega_s} \frac{\delta_{\ell\ell'}}{(2\ell + 1)\Delta\ell} \times (\tilde{C}^{im}\tilde{C}^{jn} + \tilde{C}^{in}\tilde{C}^{jm}), \quad (21)$$

where the indices i, j, \dots run over w_i and g_j , Ω_s is the survey area, $\Delta\ell$ is the width of ℓ bin, and \tilde{C} denotes the power spectrum including shot noise

$$\tilde{C}^{ij} = C^{ij} + \delta_{ij} \frac{1}{\bar{n}_i}, \quad (22)$$

where \bar{n}_i is the projected number density given by Eqs. (7) and (16).

With this covariance matrix, we can compute the Fisher matrix as

$$F_{\alpha\beta} = \sum_{\ell} \sum_{i,j,m,n} \frac{\partial C^{ij}}{\partial p_{\alpha}} [\text{Cov}(C^{ij}, C^{mn})]^{-1} \frac{\partial C^{mn}}{\partial p_{\beta}}, \quad (23)$$

where p_{α} denotes cosmological and nuisance parameters. A marginalized error on each parameter is obtained by $\sigma(p_{\alpha}) = \sqrt{(F^{-1})_{\alpha\alpha}}$.

We compute the Fisher matrix with the following setup. For the correlation among GW sources [$C^{w_i w_j}$; see Eq. (10)], while there are weak correlations between different luminosity distance bins, we ignore them and consider only correlations between the same luminosity distance bins (i.e., $C^{w_i w_j} \approx \delta_{ij} C^{w_i w_i}$). This is because such weak correlations between different bins are expected not to affect our results due to relatively large shot noise of GW sources. The correlation among spectroscopic galaxies [$C^{g_i g_j}$; see Eq. (17)] also does not have any correlation between different redshift bins. On the other hand, we consider all the combination of bins for the cross-correlation [$C^{w_i g_j}$; see Eq. (18)], given that there are large-distance correlations as shown in Fig. 1.

As stated above, observations we have in mind are the Einstein Telescope [25] for GWs and Euclid [34] for spectroscopic galaxies, although we do not tune our parameters to these surveys very carefully. We consider the redshift range of $0.3 < z < 1.5$, where the maximum redshift mainly comes from the upper limit of redshifts of the spectroscopic galaxy sample. We define luminosity distance bins of GW sources by the distance width corresponding to $\Delta z = 0.2$, and compute the minimum ($D_{i,\min}$) and maximum ($D_{i,\max}$) luminosity distances in each bin using the standard luminosity distance-redshift relation in our fiducial cosmological model. Thus we have $N_w = 6$ luminosity distance bins for GW sources. On the other hand, we define redshift bins for spectroscopic galaxies with the interval $\Delta z = 0.1$, leading to $N_g = 12$ bins. We also consider all the $N_w \times N_g$ cross-correlations for our Fisher matrix analysis. Therefore, the total number of elements of C^{ij} vector in Eq. (23) is 90. This means that the covariance matrix has the dimension 90×90 .

As for cosmological parameters, we consider h , Ω_m , and w_{de} as parameters controlling the distance-redshift relation. We also include σ_8 , which determines the normalization of power spectra, as a parameter. In addition, we include bias parameters b_{w1} , b_{w2} , b_{g1} , and b_{g2} (see Sec. III A) as nuisance parameters. In total, we have eight parameters that constitute p_{α} in Eq. (23). All the parameters are treated

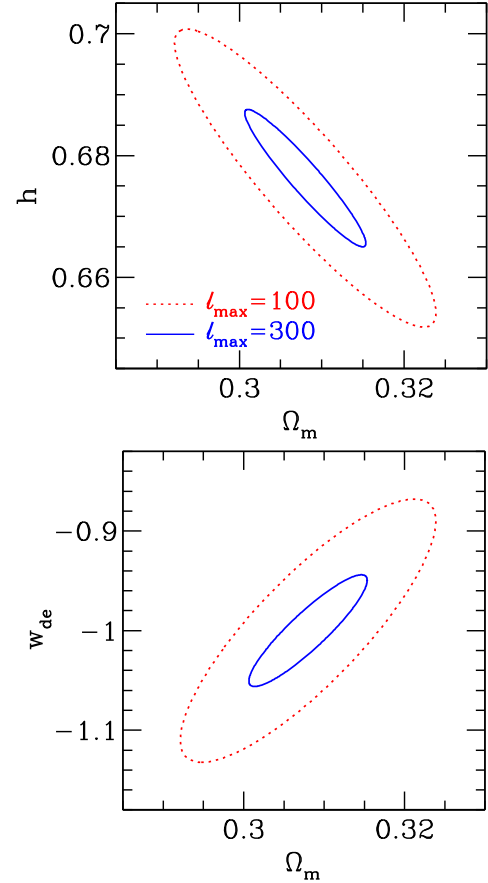


FIG. 2. Projected 68% C.L. constraints in the Ω_m - h (top) and Ω_m - w_{de} (bottom) planes. In each panel, the other model parameters are marginalized over. Solid lines show constraints for $\ell_{\text{max}} = 300$, whereas dotted lines show constraints for $\ell_{\text{max}} = 100$.

as free parameters, except σ_8 for which we add a weak prior $\sigma(\sigma_8) = 0.1$ because we find that σ_8 strongly degenerates with the bias parameters.

We consider the multipole range $10 < \ell < \ell_{\text{max}}$. The maximum multipole ℓ_{max} should be determined from the angular resolution of GW observations. The angular resolution of the Einstein telescope network corresponds to approximately $\ell_{\text{max}} = 100$ [22,35], which we adopt as a fiducial value. However we also consider an optimistic case $\ell_{\text{max}} = 300$ in order to check the dependence of our results on ℓ_{max} . Finally we assume the survey area of $\Omega_s = 15000 \text{ deg}^2$ which is covered by Euclid.

Fig. 2 shows marginalized errors on cosmological parameters for both $\ell_{\text{max}} = 100$ and $\ell_{\text{max}} = 300$. We find that tight constraints on the Hubble constant as well as dark energy parameters can be obtained from the cross-correlation analysis. The summary of constraints given in Table I indicates that a percent level constraint on the Hubble constant can be obtained, suggesting that the distance-redshift relation is successfully constrained. We also note a large improvement of constraints from $\ell_{\text{max}} = 100$ to $\ell_{\text{max}} = 300$, which implies that accurate localizations of

TABLE I. Expected marginalized errors on each cosmological parameter. See text for details.

Model	$\sigma(h)$	$\sigma(\Omega_m)$	$\sigma(w_{de})$
$\ell_{\max} = 100$	0.016	0.010	0.087
$\ell_{\max} = 300$	0.007	0.005	0.037

GW sources on the sky are crucial for the cross-correlation analysis.

The expected accuracy of cosmological parameter estimation depends on several parameters such as the number density of GW sources and their bias factors, which are poorly known. For comparison, we consider more pessimistic case with an order of magnitude smaller number density of GW sources, $T_{\text{obs}}\dot{n}_{\text{GW}} = 3 \times 10^{-7} h^3 \text{Mpc}^{-3}$, and repeat the Fisher matrix calculation. We find that the change of the expected constraint on the Hubble constant is modest, from $\sigma(h) = 0.016$ to 0.030 for $\ell_{\max} = 100$, and from $\sigma(h) = 0.007$ to 0.013 for $\ell_{\max} = 300$. This suggests that the cross-correlation technique is still useful even when the GW rate is significantly smaller than our fiducial value.

We note that the expressions of the angular power spectra in this paper have been derived using the Limber's approximation which breaks down at small ℓ [30,36]. We expect that this approximation is valid for the purpose of this paper, because the cross-correlation signal mainly comes from large ℓ , $\ell \sim \ell_{\max}$, at which the Limber's approximation is expected to be reasonably accurate for our choice of $\Delta z = 0.1$ for the spectroscopic galaxy sample. Limber's approximation becomes inaccurate for cross-correlation with large redshift differences, but due to relative large shot noise such cross-correlation does not contribute to the result very much. Although there is a long tail of cross-correlation signals toward lower redshifts (Fig. 1), it is essentially the cross-correlation of galaxies and matter at the same redshift and hence the Limber's approximation is again accurate. Nevertheless, we caution that the full calculation without the Limber's approximation may be required for more accurate predictions of the cross-correlation signals, which is beyond the scope of this paper.

IV. CONCLUSION

GWs from mergers of compact objects such as BHs serve as a useful cosmological probe because they allow us to directly measure absolute distance scales. However, in order to constrain the distance-redshift relation from GW sources we also need redshift information. While the redshift information may be obtained from observations

of EM counterparts, it is unclear whether such EM counterparts can be reliably identified, especially for BH-BH mergers. In this paper, we propose to use the cross-correlation of GW sources with spectroscopic galaxies as an alternative means of constraining the distance-redshift relation. We have explicitly included the effect of weak gravitational lensing on luminosity distance estimates in our formulation. Using the Fisher matrix formalism, we have shown that tight constraints on the Hubble constant as well as dark energy parameters can be obtained by the cross-correlation of GW sources observed by the Einstein Telescope and spectroscopic galaxies observed by Euclid.

Constraints on absolute distance scales at cosmological distances are not directly obtained except a few cases (e.g., [37–40]). GW standard sirens therefore offer invaluable information on the distance-redshift relation including the absolute distance scale. Our analysis has shown that it is possible to constrain the distance-redshift relation even without identifying EM counterparts of GW sources and thus without any redshift information on individual GW sources.

Finally we note that there is room for improving constraints on the distance-redshift relation from the cross-correlation analysis. For instance, while we have restricted our analysis to $z < 1.5$, GWs can be detected out to much higher redshifts in next-generation GW observations. For those high-redshift GWs, we can use high-redshift tracers such as quasars, or we may also be able to use galaxies with photometric redshifts for the cross-correlation analysis, if their photometric redshifts are accurate enough. For example, Euclid's near-infrared photometry, when combined with ground-based optical photometry, enables an accurate determination of photometric redshifts easily out to $z \sim 3$ [41]. Photometric galaxies are much denser and, therefore, lead to more significant detections of cross-correlation signals, which suggests that cross-correlation of GW sources with galaxies with photometric redshifts has a great potential to enhance the use of the cross-correlation method proposed in this paper. The distance-redshift relation may also be constrained by cross-correlating GW sources with tomographic weak lensing [42]. We leave exploring these possibilities for future work.

ACKNOWLEDGMENTS

I thank the anonymous referee for useful suggestions. This work was supported, in part, by the World Premier International Research Center Initiative (WPI Initiative), MEXT, Japan, and JSPS KAKENHI Grants No. 26800093 and No. 15H05892.

- [1] B. P. Abbott *et al.* (LIGO Scientific and Virgo Collaborations), *Phys. Rev. Lett.* **116**, 061102 (2016).
- [2] B. P. Abbott *et al.* (LIGO Scientific and Virgo Collaborations), [arXiv:1602.03842](https://arxiv.org/abs/1602.03842).
- [3] B. P. Abbott *et al.* (LIGO Scientific and Virgo Collaborations), *Astrophys. J.* **818**, L22 (2016).
- [4] B. F. Schutz, *Nature (London)* **323**, 310 (1986).
- [5] D. E. Holz and S. A. Hughes, *Astrophys. J.* **629**, 15 (2005).
- [6] N. Dalal, D. E. Holz, S. A. Hughes, and B. Jain, *Phys. Rev. D* **74**, 063006 (2006).
- [7] C. Cutler and D. E. Holz, *Phys. Rev. D* **80**, 104009 (2009).
- [8] S. Nissanke, D. E. Holz, S. A. Hughes, N. Dalal, and J. L. Sievers, *Astrophys. J.* **725**, 496 (2010).
- [9] C. Shapiro, D. Bacon, M. Hendry, and B. Hoyle, *Mon. Not. R. Astron. Soc.* **404**, 858 (2010).
- [10] C. M. Hirata, D. E. Holz, and C. Cutler, *Phys. Rev. D* **81**, 124046 (2010).
- [11] S. Hilbert, J. R. Gair, and L. J. King, *Mon. Not. R. Astron. Soc.* **412**, 1023 (2011).
- [12] A. Nishizawa, A. Taruya, and S. Saito, *Phys. Rev. D* **83**, 084045 (2011).
- [13] S. R. Taylor and J. R. Gair, *Phys. Rev. D* **86**, 023502 (2012).
- [14] N. Tamanini, C. Caprini, E. Barausse, A. Sesana, A. Klein, and A. Petiteau, [arXiv:1601.07112](https://arxiv.org/abs/1601.07112).
- [15] S. Camera and A. Nishizawa, *Phys. Rev. Lett.* **110**, 151103 (2013).
- [16] M. Arabsalmani, V. Sahni, and T. D. Saini, *Phys. Rev. D* **87**, 083001 (2013).
- [17] V. Connaughton *et al.*, [arXiv:1602.03920](https://arxiv.org/abs/1602.03920).
- [18] A. Loeb, *Astrophys. J.* **819**, L21 (2016).
- [19] A. Nishizawa, K. Yagi, A. Taruya, and T. Tanaka, *Phys. Rev. D* **85**, 044047 (2012).
- [20] N. Seto, S. Kawamura, and T. Nakamura, *Phys. Rev. Lett.* **87**, 221103 (2001).
- [21] C. Messenger and J. Read, *Phys. Rev. Lett.* **108**, 091101 (2012).
- [22] T. Namikawa, A. Nishizawa, and A. Taruya, *Phys. Rev. Lett.* **116**, 121302 (2016).
- [23] J. A. Newman, *Astrophys. J.* **684**, 88 (2008).
- [24] P. A. R. Ade *et al.* (Planck Collaboration), [arXiv:1502.01589](https://arxiv.org/abs/1502.01589).
- [25] M. Punturo *et al.*, *Classical Quantum Gravity* **27**, 194002 (2010).
- [26] M. Dominik, K. Belczynski, C. Fryer, D. E. Holz, E. Berti, T. Bulik, I. Mandel, and R. O’Shaughnessy, *Astrophys. J.* **779**, 72 (2013).
- [27] T. Kinugawa, K. Inayoshi, K. Hotokezaka, D. Nakauchi, and T. Nakamura, *Mon. Not. R. Astron. Soc.* **442**, 2963 (2014).
- [28] K. Belczynski, D. E. Holz, T. Bulik, and R. O’Shaughnessy, [arXiv:1602.04531](https://arxiv.org/abs/1602.04531).
- [29] D. N. Limber, *Astrophys. J.* **119**, 655 (1954).
- [30] M. LoVerde and N. Afshordi, *Phys. Rev. D* **78**, 123506 (2008).
- [31] M. Oguri and M. Takada, *Phys. Rev. D* **83**, 023008 (2011).
- [32] D. J. Eisenstein and W. Hu, *Astrophys. J.* **496**, 605 (1998).
- [33] R. Takahashi, M. Sato, T. Nishimichi, A. Taruya, and M. Oguri, *Astrophys. J.* **761**, 152 (2012).
- [34] R. Laureijs *et al.* (EUCLID Collaboration), [arXiv:1110.3193](https://arxiv.org/abs/1110.3193).
- [35] T. Sidery *et al.*, *Phys. Rev. D* **89**, 084060 (2014).
- [36] D. Jeong, E. Komatsu, and B. Jain, *Phys. Rev. D* **80**, 123527 (2009).
- [37] M. Oguri, *Astrophys. J.* **660**, 1 (2007).
- [38] S. H. Suyu *et al.*, *Astrophys. J.* **766**, 70 (2013).
- [39] D. J. Eisenstein *et al.* (SDSS Collaboration), *Astrophys. J.* **633**, 560 (2005).
- [40] L. Anderson *et al.* (BOSS Collaboration), *Mon. Not. R. Astron. Soc.* **441**, 24 (2014).
- [41] F. B. Abdalla, A. Amara, P. Capak, E. S. Cypriano, O. Lahav, and J. Rhodes, *Mon. Not. R. Astron. Soc.* **387**, 969 (2008).
- [42] W. Hu, *Astrophys. J.* **522**, L21 (1999).